ISSN 1330-3651 (Print), ISSN 1848-6339 (Online)
https://doi.org/10.17559/TV-20191021140800
Original scientific paper

Application of Fracture Mechanics Parameters to Spherical Storage Tank Integrity Assessment

Aleksandar MILOVANOVIĆ*, Aleksandar SEDMAK, Nebojsa GNJATOVIĆ

Abstract: Fracture mechanics parameters have been applied to assess pressure vessel integrity. The pressure vessel analysed here was the ammonia spherical tank (volume of 1800 m^3, outer diameter 15.12 m, thickness 30 mm) where different cracks in the longitudinal and transverse butt joints were found. The finite element method was used to calculate stress and strain state and to analyse cracks and their influence on spherical storage tank integrity. Toward this end, the stress intensity factors were analytically determined, and compared with the fracture toughness to find out the critical pressure using Failure Assessment Diagram (FAD) in combination with net stress vs. critical stress.

Keywords: failure assessment diagram; finite element method; spherical storage tank; stress intensity factor; structure integrity

1 INTRODUCTION

The spherical storage tank for ammonia (volume 1800 m^3, outer diameter D_s = 15.12 m and thickness s_e = 30 mm), made of high strength low alloyed steel A36.52 (NIOVAL 47), was tested recently using non-destructive techniques (NDT). The maximum operational pressure was p = 16 bar, whereas test pressure was 30% higher, p_i = 20.8 bar. A large number of surface cracks were detected in welded joints, and four critical ones were analysed in this paper, no. 204, 205, 207 and 211, Fig. 1. As explained in [1], it was decided not to repair the storage tank, because of previous experience, indicating that more damage than benefit would be made, [2, 3], mainly due to unfavourable microstructure of the steel, used for tank production, [4]. Namely, more cracks were found after repair welding than before, not only because of material, but even more important, due to unnecessary over-pressurizing during testing, [5, 6].

Therefore, another strategy was used here, based on structural integrity assessment, enabling simple treatment/removal of cracks with a profile milling cutter. Toward this end, the stress intensity factors for detected cracks were calculated and compared with the fracture toughness to assess spherical storage tank structural integrity. Final decision is based on an application of Failure Analysis Diagram (FAD), i.e. combination of brittle fracture and plastic collapse, [7-10].

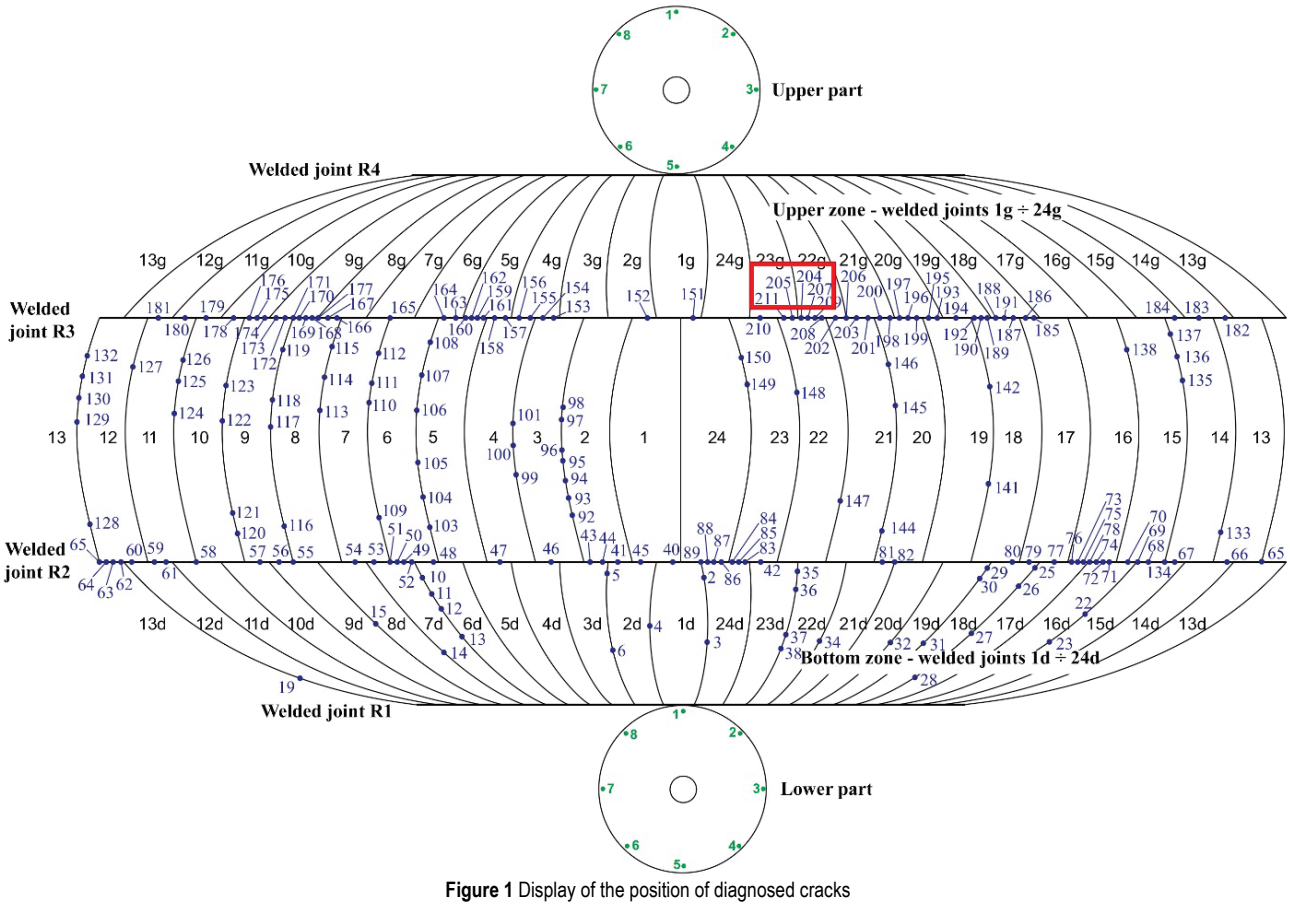

Figure 1 Display of the position of diagnosed cracks

2 CALCULATION OF THE SPHERICAL TANK WALL THICKNESS USING EN 13445-3:2017

Spherical tank is made of A36.52 [1], with chemical composition and mechanical properties given in Tab. 1 and Tab. 2, respectively.

Table 1 Chemical composition in %

Designation	C	Mn	Si	P_{max}	S_{max}	Al_{total}	Cr	Mo	V
A36.52	≤0.157	1.39	0.3	0.013	0.021	≥0.015	0.08	0.02	0.08

Table 2 Mechanical properties

Designation	Standard	Thickness / mm	$R_{p0.2t}$ / MPa	R_m / MPa	Elong. ε / %	Toughness KV $(J)_{min}$		
A36.52	AFNOR	≤ 50	360	520	23	−20°	0°	+20°
						47	-	-

According to EN 13445-3 the allowed stress for steel A36.52 is σ_{all} = 240 MPa or 360 MPa, for local conditions, [1]. In that case, minimum thickness for a spherical shell under pressure, p = 16 bar, is t = 26.2 mm, [1].

3 ASSESSMENT OF THE INTEGRITY OF THE SPHERICAL TANK USING FRACTURE MECHANICS PARAMETERS

During regular periodic inspection of transversal and longitudinal welded joints of the segments of the spherical storage tank for storing liquid ammonia by non-destructive methods, 211 irregularities were detected in the form of unacceptable defects (cracks). Technical regulations do not allow the use of pressure equipment with such defects. Anyhow, since eventual repair would make more damage than benefit, [11, 12], these defects were analysed by fracture mechanics using a conservative approach to prove pressure vessel integrity. To calculate stress intensity factors one has to know load and geometry. If the fracture toughness cannot be measured, a conservative value can be used instead, [7, 9]. Corrosion and fatigue, as well as residual stresses and proximity of the connections are also taken into account. As the most critical, cracks no. 204, 205, 207 and 211 have been analysed by fracture mechanics principles. The position of detected errors is schematically shown in Fig. 1.

Application of linear elastic fracture mechanics is based on the stress intensity factor, K_I, representing load and geometry, including shape and size of crack, on one hand, whereas its critical value, i.e. fracture toughness, K_{Ic}, represents the material resistance to crack growth. Using this interpretation, structure integrity is established as follows:

$K_I \leq K_{Ic}$ - the structure integrity is not compromised,

$K_I > K_{Ic}$ - the structure integrity is jeopardized because of possible brittle fracture.

Data for cracks no. 204 and 205 is:

- vessel geometry (thickness t = 27.5 mm, mean radius R_{sr} = 7545.5 mm),
- crack geometry (length l = 30 mm, depth a = 1.5 mm, location - the transverse butt welded joint R3),
- load (internal pressure p = 16 bar, residual stress σ_R = 0 MPa),
- weld metal fracture toughness 1560 MPa√mm, taken as the conservative, i.e. minimum value, according to testing performed in [4].

Now, for the stress intensity factor one gets:

$$K_I = \left(\frac{p \cdot R_{sr}}{2 \cdot t} + \sigma_R \right) \cdot \sqrt{\pi \cdot a} = 476.5 \text{ MPa} \sqrt{\text{mm}} \quad (1)$$

which is 30.5% of the critical value (K_{Ic} = 1560 MPa√mm), used as the minimum fracture toughness in the most critical weldment zone (HAZ), [7,9].

Data for the crack no. 207 is:

- vessel geometry (thickness t = 27 mm, mean radius R_{sr} = 7545.5 mm),
- crack geometry (length l = 25 mm, depth a = 2 mm, location - the transverse butt welded joint R3),
- load (internal pressure p = 16 bar, residual stress σ_R = 0 MPa),
- weld metal fracture toughness 1560 MPa√mm, taken as the conservative value.

For the stress intensity factor the following is obtained:

$$K_I = \left(\frac{p \cdot R_{sr}}{2 \cdot t} + \sigma_R \right) \cdot \sqrt{\pi \cdot a} = 560.41 \text{ MPa} \sqrt{\text{mm}} \quad (2)$$

which is far below the critical value (K_{Ic} = 1560 MPa√mm), i.e. 35.9% of it.

Data relevant for the crack no. 211 analysis are:

- vessel geometry (thickness t = 25 mm, mean radius R_{sr} = 7545.5 mm),
- crack geometry (length l = 60 mm, depth a = 4 mm, location - the transverse butt welded joint R3),
- load (internal pressure p = 16 bar, residual stress σ_R = 0 MPa),
- fracture toughness of the weld metal 1560 MPa√mm, taken as the minimum value.

Now, for the stress intensity factor one gets:

$$K_I = \left(\frac{p \cdot R_{sr}}{2 \cdot t} + \sigma_R \right) \cdot \sqrt{\pi \cdot a} = 855.94 \text{ MPa} \sqrt{\text{mm}} \quad (3)$$

which is well below the critical value (K_{Ic}=1560 MPa√mm), i.e. 54.9% of it.

Further analysis of cracks no. 204, 205, 207 and 211 can be illustrated with the Failure Assessment Diagram (FAD). It is necessary to specify parameters K_r and S_r. Parameter K_r is determined according to the presented equation:

$$K_r = K_I / K_{IC} \quad (4)$$

Parameter Sr is determined according to:

$$S_r = \frac{\sigma_n}{\sigma_F} = \frac{\frac{p \cdot R_{sr}}{2 \cdot t}}{\frac{R_{p0.2} + R_m}{2}} \quad (5)$$

Parameters K_r and S_r for crack no. 204 and 205 are:

$$K_r = K_I / K_{IC} = 0.3 \quad (6)$$

$$S_r = \frac{\sigma_n}{\sigma_F} = \frac{\frac{p \cdot R_{sr}}{2 \cdot t}}{\frac{R_{p0,2} + R_m}{2}} = 0.5 \quad (7)$$

Parameters K_r and S_r for crack no. 207 are:

$$K_r = K_I / K_{IC} = 0.36 \quad (8)$$

$$S_r = \frac{\sigma_n}{\sigma_F} = \frac{\frac{p \cdot R_{sr}}{2 \cdot t}}{\frac{R_{p0,2} + R_m}{2}} = 0.51 \quad (9)$$

Parameters K_r and S_r for crack no. 211 are:

$$K_r = K_I / K_{IC} = 0.55 \quad (10)$$

$$S_r = \frac{\sigma_n}{\sigma_F} = \frac{\frac{p \cdot R_{sr}}{2 \cdot t}}{\frac{R_{p0.2} + R_m}{2}} = 0.55 \quad (11)$$

Based on the values obtained for the parameters K_r and S_r for cracks no. 204, 205, 207 and 211 in the Failure Assessment Diagram points are located in the secure part of the diagram shown in Fig. 2.

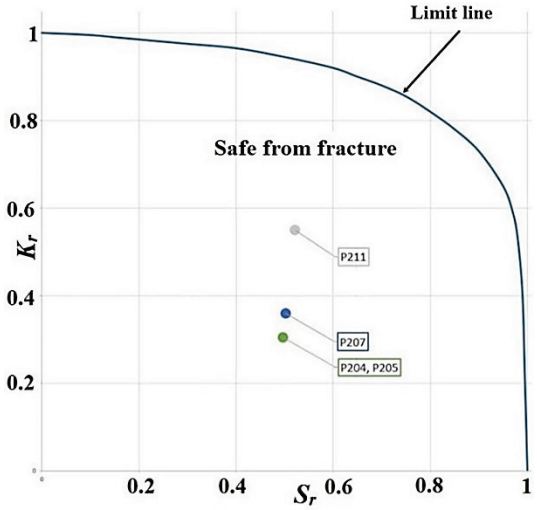

Figure 2 Failure Assessment Diagram for cracks no. 204, 205, 207 and 211

A critical value of crack depth, i.e. the depth at which the stress intensity factor K_I reaches its critical value K_{Ic}, is a_{cr} = 8.8 mm.

4 Finite Element Model and Influence of Processed Cracks on the Stress State

The finite element model of the ammonia spherical tank containing cracks has to be three-dimensional (3D) because of complex geometry. The maximum length for forming the finite element model is calculated using EN 13445: 3-2017, [13-15]:

$$l_{so} = \sqrt{(2 \cdot r_{is} + e_{as}) \cdot e_{as}} = 661.54 \text{ mm} \quad (12)$$

where: $r_{is} = D_e/2 - e_{as}$ = 7531 mm - mean radius of the sphere, $e_{as} = s_e - c - \delta_e = 30 - 1 - 0 = 29$ mm - thickness reduced by values of c and δ_e. Fig. 3 presents the 3D model, indicating crack no. 204 dimensions.

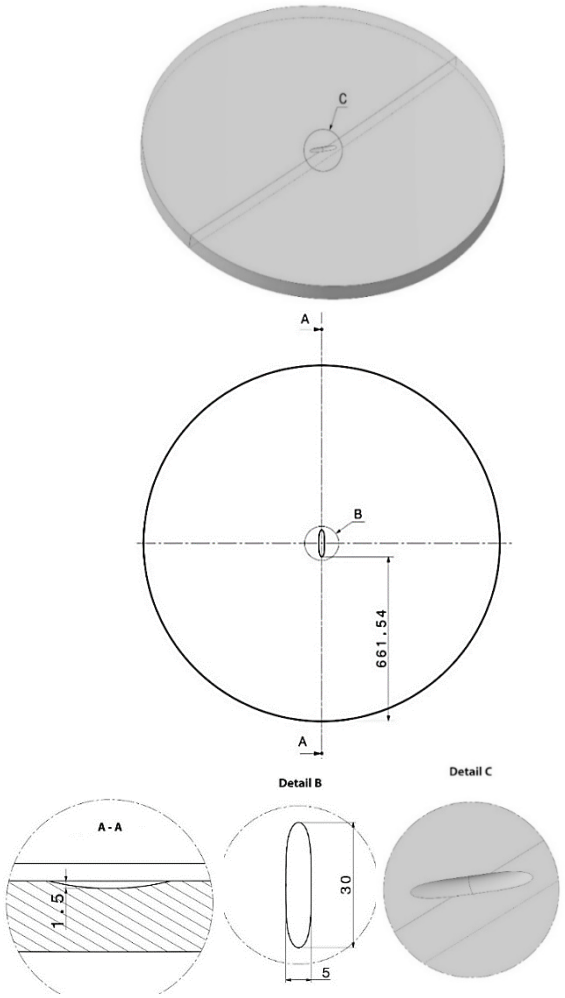

Figure 3 3D model

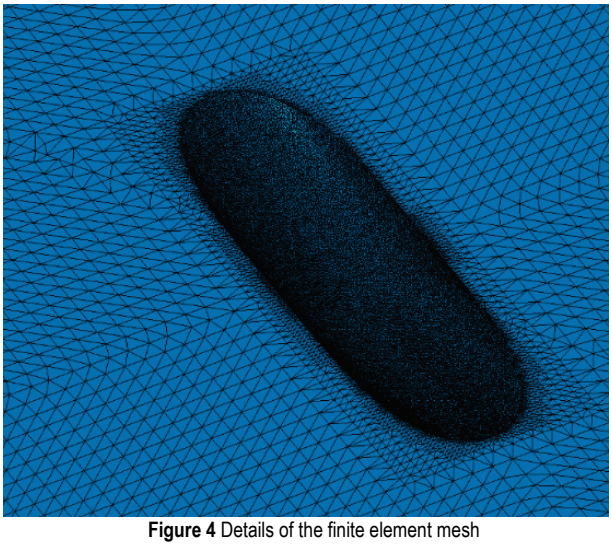

Figure 4 Details of the finite element mesh

The finite element mesh consists of 2.558.929 tetrahedron-type elements and 544.427 nodes. Finite element size in crack zone is 0.2 mm, and on the part of the spherical shell

without a crack, 2 mm. Some details of the finite elements mesh in the spherical shell crack zone are shown in Fig. 4.

The effect of cracks on the spherical tank stresses and strains was simulated by a groove, introduced following the real procedure of taking crack out. Loading was uniform pressure equal to the maximum value of the hydrostatic pressure (p = 16 bar) plus maximum calculated value for the groove. Tab. 3 presents the dimensions of grooves at locations of the cracks and values of maximum stresses.

Table 3 Dimensions of grooves and maximum stress values

Defect	Groove dimensions $l \times b \times a$ / mm	Maximum stress / MPa	Corrected dimension $l \times b \times a$ / mm	Maximum stress / MPa
204	30 × 5 × 1.5	382.7	30 × 10 × 1.5	298.6
205	30 × 5 × 1.5	382.7	30 × 10 × 1.5	298.6
207	25 × 5 × 2	429.5	25 × 10 × 2	326.2
211	60 × 15 × 4	380.8	60 × 25 × 4	325.9

Figs. 5, 6 and 7 define stresses in the groove zone, indicating maximum stress, $\sigma_{max,s}$ = 382.7 MPa, Fig. 5a, at the bottom of groove no. 204 and 205, where the thickness is reduced from 30 mm to 28.5 mm, which is larger than the allowed local stress σ_{all} = 360 MPa. As the stress proof is not satisfied, the groove dimensions have to be corrected, to reduce the maximum stress to $\sigma_{max,s}$ = 298.6 MPa, Fig. 5b.

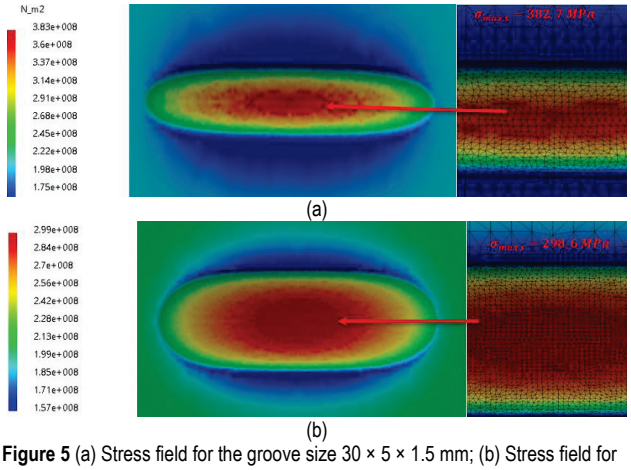

Figure 5 (a) Stress field for the groove size 30 × 5 × 1.5 mm; (b) Stress field for the corrected groove size 30 × 10 × 1.5 mm

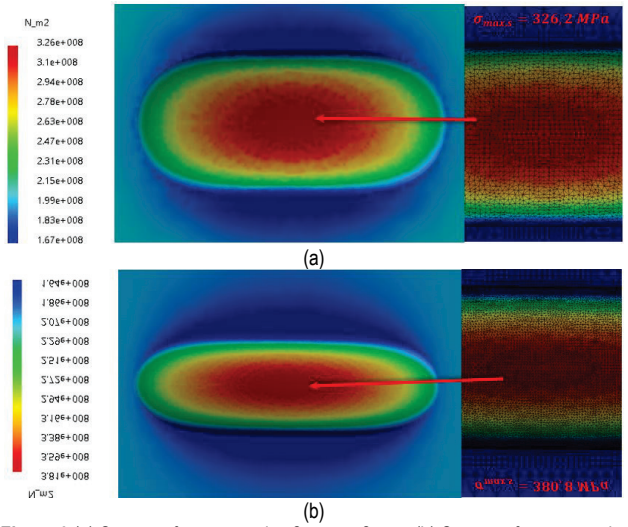

Figure 6 (a) Stresses for groove size 25 × 5 × 2 mm; (b) Stresses for corrected groove size 25 × 10 × 2 mm

Maximum stress at the bottom of the groove no. 207 (thickness reduced from 30 mm to 28 mm is $\sigma_{max,s}$ = 429.5 MPa, which is larger than the allowed local stress σ_{all} = 360 MPa, Fig. 6a. Therefore, groove dimensions were corrected to reduce the maximum stress to $\sigma_{max,s}$ = 326.2 MPa, Fig. 6b.

Maximum stress at the bottom of the groove no. 211 (thickness reduced from 30 mm to 26 mm) is $\sigma_{max,s}$ = 380.8 MPa, which is larger than the allowed local stress σ_{all} = 360 MPa, Fig. 7a. Therefore, groove dimensions were corrected to reduce the maximum stress to $\sigma_{max,s}$ = 325.9 MPa, Fig. 7b.

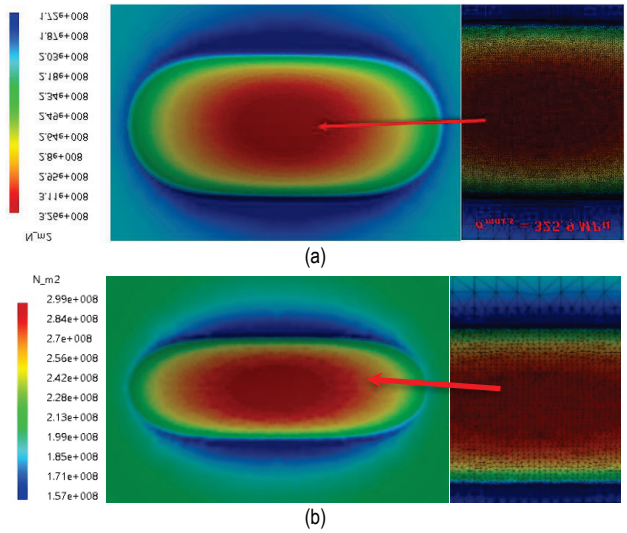

Figure 7 (a) Stresses for groove size 60 × 15 × 4 mm; (b) Stresses for corrected groove size 60 × 25 × 4 mm

4 CONCLUSIONS

Calculation of the spherical tank thickness according to EN 13445-3:2017 is satisfied since all the required thicknesses are greater than the minimum measured thickness. Using fracture mechanics parameters, it was concluded that detected defects do not affect spherical storage tank integrity. Also by using fracture mechanics parameters, the value of the critical error depth was determined which would bring the spherical tank integrity in critical state. By checking the maximum stress in corrected zones using the finite element method it was concluded that the integrity of the spherical storage tank will not be affected at the defined dimensions of the groove.

8 REFERENCES

[1] Milovanović, A. & Sedmak, A. (2018). Integrity assessment of ammonia spherical storage tank. *Procedia Structural Integrity, 13*, 994-999. https://doi.org/10.1016/j.prostr.2018.12.185

[2] Sedmak, S. & Sedmak, A. (2005). Integrity of Penstock of Hydroelectric Power plant. *Structural Integrity and Life, 5*(2), 59-70.

[3] Sedmak, A., Sedmak, S., & Milović, Lj. (2011). Pressure equipment integrity assessment by elastic-plastic fracture mechanics. *Society for Structural Integrity and Life.*

[4] Tuma, J. V. & Šuštarčić, B. (2013). Fracture Mechanics Investigations of Structural Steels with the Yield Stresses between 265 and 1000 MPa, ESIS CP2006.

[5] Golubovic, T., Sedmak, A., Spasojević-Brkić, V., Kirin, S., Mijatović, T., & Martić, I. (2018). Risk based structural integrity assessment of a vinyl-chloride monomer storage

tank with crack-like defects. *Hemijska industrija*, 72(4), 177-182. https://doi.org/10.2298/HEMIND171009006G
[6] Sedmak, A., Algool, M., Kirin, S., Rakicevic, D., & Bakic, R. (2016). Industrial safety of pressure vessels - Structural integrity point of view. *Hemijska industrija, 70*(6), 685-694. https://doi.org/10.2298/HEMIND150423005S
[7] Golubovic, T., Sedmak, A., Spasojević Brkić, V., Kirin, S., & Rakonjac, I. (2018). Novel risk based assessment of pressure vessels integrity. *Technical Gazette, 25*(3), 803-807. https://doi.org/10.17559/TV-20170829144636
[8] Vučetić, I., Kirin, S., Vučetić, T., Golubović, T., & Sedmak, A. (2018). Risk Analysis in the Case of Air Storage Tank Failure at RHPP Bajina Bašta. *Structural Integrity and Life, 18*(1), 3-6.
[9] Martic, I., Sedmak, A., Mitrovic, N., Sedmak, S. A., & Vucetic, I. (2019). Effect of over-pressure on pipeline structural integrity. *Technical Gazette, 26*(3), 852-855.
[10] Radu, D., Sedmak, A., Sedmak, S. A., & Dunjic, M. Stress analysis of steel structure comprising cylindrical shell with billboard tower. *Technical Gazette, 25*(2), 429-436. https://doi.org/10.17559/TV-20160819201538
[11] Jovičić, R., Radaković, Z., Petronić, S., Džindo, E., & Jovičić Bubalo, K. (2016). Inspection, Non-Destructive Tests and Repair of Welded Pressure Equipment. *Structural Integrity and Life, 16*(3), 187-192.
[12] Jovičić, R., Petronić, S., Sedmak, S., Tatić, U., & Jovičić, K. (2013). Integrity Assessment of Tanks with Microcracks in Welded Joints. *Structural Integrity and Life, 13*(2), 131-136.
[13] EN 13445-3:2014 Unfired pressure vessels - Part 3: Design
[14] Milovanović, A., Sedmak, A., Tomić, R., Hot, I., & Martić, I. (2016). Calculation of local loads in torispherical end of vertical vessel with skirt according to EN 13445-3:2014. *Structural Integrity and Life, 16*(1), 53-58.
[15] Martić, I., Sedmak, A., Tomić, R., & Hot, I. (2016). Remaining life determination for pressure vessel in a refinery. *Structural Integrity and Life, 16*(1), 49-58.

Contact information:

Aleksandar MILOVANOVIĆ
(Corresponding author)
Faculty of Mechanical Engineering,
Kraljice Marije 16, 11000 Belgrade, Serbia
E-mail: amilovanovic@mas.bg.ac.rs

Aleksandar SEDMAK
Faculty of Mechanical Engineering
Kraljice Marije 16, 11000 Belgrade, Serbia
E-mail: asedmak@mas.bg.ac.rs

Nebojša GNJATOVIĆ
Faculty of Mechanical Engineering,
Kraljice Marije 16, 11000 Belgrade, Serbia
E-mail: ngnjatovic@mas.bg.ac.rs